

European Journal of Pharmacology

Molecular and cellular pharmacology

Research paper

Gadolinium modulates gentamicin uptake via an endocytosis-independent pathway in HK-2 human renal proximal tubular cell line

Takeshi Sawada, Junya Nagai, Yumi Okada, Ryoko Yumoto, Mikiyoshi Takano*

*Department of Pharmaceutics and Therapeutics, Graduate School of Biomedical Sciences,
Hiroshima University, 1-2-3 Kasumi, Minami-ku, Hiroshima 734-8553, Japan*

*Corresponding author. Department of Pharmaceutics and Therapeutics,
Graduate School of Biomedical Sciences, Hiroshima University, 1-2-3 Kasumi, Minami-ku,
Hiroshima 734-8553, Japan.

Tel. +81-82-257-5315; Fax. +81-82-257-5319

E-Mail: takanom@hiroshima-u.ac.jp

Abstract

The aim of this study was to characterize the uptake mechanism of gentamicin, an aminoglycoside antibiotic, in human renal proximal tubular cell line HK-2. Sodium-dependent uptake of D-[^3H]glucose and L-[^3H]alanine was observed in HK-2 cells, indicating that the cells employed in this study retain functional characteristics of the renal proximal tubular cells. On the other hand, mRNA and protein expression of megalin, an endocytic receptor which is responsible for the internalization of gentamicin into the renal proximal tubular cells, was very faint in HK-2 cells. Various aminoglycoside antibiotics including amikacin and kanamycin inhibited the uptake of [^3H]gentamicin. Colchicine and cytochalasin D, general endocytosis inhibitors, had no significant effect on [^3H]gentamicin uptake in HK-2 cells, which was in contrast to the results observed in OK cells, a renal proximal tubular cell line expressing megalin. Furthermore, unlike OK cells, [^3H]gentamicin uptake in HK-2 cells was not inhibited by N-WASP181-200, a cationic 20-amino acid peptide. Ruthenium red, a nonspecific cation channel blocker, decreased the uptake of [^3H]gentamicin in HK-2 cells. In contrast, the trivalent cation gadolinium biphasically modulated [^3H]gentamicin uptake with a maximum increase at 0.3 mM gadolinium. The enhanced effect of gadolinium on [^3H]gentamicin uptake was independent of gadolinium-induced increase in intracellular calcium concentration. These findings indicate that gentamicin is primarily taken up via an endocytosis-independent pathway in HK-2 cells with very low expression of megalin, and that the uptake of gentamicin is modulated by gadolinium.

Key words: Gentamicin, HK-2 cells, Renal proximal tubular cells, Cellular uptake, Endocytosis-independent pathway, Gadolinium

1. Introduction

Aminoglycoside antibiotics such as gentamicin and amikacin are used worldwide in the treatment of Gram-negative infections. However, serious complications like nephrotoxicity and ototoxicity are dose-limiting factors in the clinical use of aminoglycosides. A relative large amount of the intravenously or intramuscularly administered dose is accumulated in the kidney (about 10% of dose), while little distribution is observed in other tissues. Aminoglycosides remain with a relatively long half-life in the renal proximal tubule, which subsequently induce renal damages. Thus, aminoglycoside-induced nephrotoxicity is considered to be directly related to the concentrated accumulation of the drug in the renal proximal tubular cells (Mingeot-Leclercq and Tulkens, 1999; Nagai and Takano, 2004; Servais et al., 2008; Lopez-Novoa et al., 2011).

In earlier studies, aminoglycosides were shown to bind to various acidic phospholipids, but not to neutral phospholipids (Schacht, 1979; Sastrasinh et al., 1982). Furthermore, increase in apical phosphatidylinositol was associated with increased apical gentamicin binding under ischemic conditions (Molitoris et al., 1993). Subsequently, Moestrup et al. (1995) reported that gentamicin binds to an endocytic receptor megalin. Megalin is abundantly expressed in S1 and S2 segments of rat renal proximal tubules (Christensen et al., 1995), where aminoglycosides are highly accumulated (Vandewalle et al., 1981; Wedeen et al., 1983). We previously reported that there was a good relationship between megalin level and renal accumulation of aminoglycosides using maleate-treated rats (Nagai et al., 2001). Furthermore, megalin knockout mice showed a dramatic decrease in gentamicin accumulation in the kidney (Schmitz et al., 2002). Such a role of megalin in renal uptake of aminoglycosides might, at least in part, explain the observations

that gentamicin is taken up by an endocytosis pathway in LLC-PK₁ pig kidney epithelial cell line (Hori et al., 1992; Takano et al., 1994), expressing megalin (Nielsen et al., 1998).

Myrdal et al. (2005) reported the intracellular distribution of Texas-Red labeled gentamicin (GTTR) in opossum kidney (OK) cells established from the renal proximal tubule and Madin-Darby canine kidney (MDCK) cells established from the renal distal tubule. According to the report, GTTR was present in cytoplasmic and nuclear compartments before the fluorescence was detected in endosomes. Therefore, the cytoplasmic uptake of GTTR may occur via an endocytosis-independent pathway such as ion channels, transporters or pores. Furthermore, the cellular uptake of GTTR has been reported to be mediated by members of transient receptor potential (TRP) cation channels including TRPV1, TRPV4 and TRPA1 (Myrdal and Steyger, 2005; Karasawa et al., 2008; Stepanyan et al., 2011).

The human renal proximal cell line HK-2, derived from normal kidney of an adult male, retains morphological and biochemical characteristics of renal proximal tubular cells (Ryan et al., 1994). Therefore, HK-2 cells have been widely used as an in vitro model for studies on nephrotoxicity induced by various endogenous and exogenous compounds (Iwata and Zager, 1996; Zager et al., 2007; Li et al., 2008; Park et al., 2010). However, the transport mechanism of aminoglycosides in HK-2 cells has not been clarified yet. In this study, we characterized the cellular uptake of [³H]gentamicin in HK cells.

2. Materials and methods

2.1. Materials

[³H]Gentamicin sulfate (7.4 GBq/g) was obtained from American Radiolabeled Chemicals (St. Louis, MO, USA). D-[2-³H]glucose (310.8 GBq/mmol) and L-[2,3-³H]alanine (1.83 TBq/mmol) were purchased from Moravek Biochemicals, Inc. (Bera, CA, USA). Unlabeled gentamicin sulfate, neomycin sulfate, kanamycin monosulfate, 2,4-dinitrophenol, gadolinium chloride, ruthenium red and Fura-2 AM were obtained from Nacalai Tesque (Kyoto, Japan). Streptomycin sulfate, amikacin sulfate, tobramycin sulfate, colchicine were purchased from Sigma-Aldrich (St. Louis, MO, USA). Sodium azide was obtained from Katayama Chemical Industries Co., Ltd. (Osaka, Japan). Arbekacin sulfate was from Meiji Seika Kaisha, Ltd (Tokyo, Japan). 2-deoxy-D-glucose was purchased from Kanto Chemical Co. Inc. (Tokyo, Japan). Cytochalasin D was purchased from Wako Pure Chemical Industries, Ltd. (Osaka, Japan). N-WASP181-200 (NISHTKEKKKGKKKKKRLTK) was chemically synthesized with a peptide synthesizer as described previously (Watanabe et al., 2004). All other chemicals used in the experiments were commercial products of the highest purity available.

2.2. Cell culture

HK-2 cells, a human proximal tubular cell line, were purchased from American Type Culture Collection (Manassas, VA, USA). The cells were cultured in Dulbecco's modified Eagle's medium/Nutrient Mixture F-12 Ham (Sigma-Aldrich) containing 10% fetal bovine serum in an atmosphere of 5% CO₂-95% air at 37°C, and were subcultured every 7 days using 0.02% EDTA

and 0.05% trypsin. Rat yolk sac carcinoma cell line (L2) was cultured in Dulbecco's modified Eagle medium (Invitrogen, Carlsbad, CA, USA) containing 10% fetal bovine serum without antibiotics in an atmosphere of 5% CO₂-95% air at 37°C, and were subcultured every 3-5 days using 0.02% EDTA and 0.05% trypsin. Fresh medium was replaced every 2 days, and the cells were used for the experiments on 4 days after seeding. OK cells were cultured in medium 199 (Gibco BRL, Life Technologies, Grand Island, NY, USA) containing 10% fetal bovine serum without antibiotics, in an atmosphere of 5% CO₂-95% air at 37 °C, and subcultured every 7 days using 0.02% EDTA and 0.05% trypsin.

2.3. Uptake studies

Uptake studies were performed in the confluent cells attached to the 24-well plates. Briefly, fresh medium was replaced every 2 days, and the cells were used on the 5-7 days after seeding. Experiments were performed in Dulbecco's phosphate buffered saline (PBS buffer containing in mM, 137 NaCl, 3 KCl, 8 Na₂HPO₄, 1.5 KH₂PO₄, 1 CaCl₂ and 0.5 MgCl₂). PBS buffer containing 5 mM D-glucose (PBS(G) buffer) was used as an incubation buffer. In Na⁺-free conditions, choline chloride and K₂HPO₄ in PBS(G) buffer were substituted for NaCl and Na₂HPO₄, respectively. After removal of the culture medium, each well was washed and preincubated with PBS(G) buffer. Then, PBS(G) buffer containing [³H]gentamicin, D-[³H]glucose or L-[³H]alanine was added to each well, and the cells were incubated at 37°C or 4°C for a specified period. The conditions for cell treatment with inhibitors were described below. When the effects of gadolinium and/or ruthenium red were examined, HEPES buffer (in mM, 140 NaCl, 10 KCl, 20 HEPES, 1 CaCl₂, 0.5 MgCl₂, 5 glucose; pH 7.4 with NaOH solution) was used as an incubation buffer, instead of PBS(G) buffer in order to prevent crystallization. At the

end of the incubation, the cells were rinsed rapidly three times with 1 ml of ice-cold PBS buffer. Then, the cells were scraped with a cell scraper into 0.3 ml of the ice-cold PBS buffer, and the cells were washed again with 0.3 ml of the ice-cold PBS buffer to improve the recovery of the cells. The cells were centrifuged at 4°C for 5 min at 7,043 g and the supernatant was discarded. The cell pellet was resuspended gently in 0.3 ml of the ice-cold PBS buffer and centrifuged again. The pellet was suspended in 0.1 M NaOH, and the amount of radioactive substrate taken up by the cells was measured by a liquid scintillation counting method. Protein content was analyzed by Bradford method with bovine serum albumin as a standard (Bradford 1976). The uptake of radioactive substrate was normalized for the protein content of the cells in each well.

2.4. Cell treatment

Stock solution of cytochalasin D was prepared in dimethyl sulfoxide (DMSO) at concentrations of 5 mM and was kept in a freezer until used. Other inhibitors were dissolved on the day of each experiment. Sodium azide and 2,4-dinitrophenol were prepared in PBS(G) buffer. Gadolinium and ruthenium red were prepared in HEPES buffer. Colchicine was dissolved in DMSO. The final concentration of DMSO in the incubation buffer was less than 0.5%. The control cells were treated with the same concentration of DMSO in each experiment. The pretreatment period for each inhibitor was 15 min (sodium azide or 2,4-dinitrophenol) or 120 min (cytochalasin D or colchicine). Thereafter, the cells were incubated for a stated period with PBS(G) or HEPES buffer containing radioactive substrate with or without each inhibitor.

2.5. RT-PCR analysis

Total RNA from HK-2 cells was extracted using RNeasy[®]Plus Mini Kit (QIAGEN GmbH, Hilden, Germany). RT-PCR was performed using a ReverTra Dash RT-PCR kit (TOYOBO Co., LTD., Osaka, Japan). The primer pair of megalin sense and antisense (sense: 5'-TAAGTCAGTGCCCAACCTTT-3'; anti-sense: 5'-GCGGTTGTTCTGGAG-3') was specific for a 291-bp fragment of megalin transcripts. The primer pair of sodium-glucose cotransporter subtype 2 (SGLT2) sense and antisense (sense: 5'-CTTCACCATGGACATCTACACG-3'; anti-sense: 5'-CAGCACAATGGCGAAGTAGA-3') was specific for a 388-bp fragment of SGLT2 transcripts. The primer pair of chloride channel 5 (ClC-5) sense and antisense (sense: 5'-ACCATGAACATTGTTGCTGGAAC-3'; anti-sense: 5'-CTGCCAGCACCAAGGTGATGG-3') was specific for a 315-bp fragment of ClC-5 transcripts. The PCR conditions consisted of an initial denaturation at 94 °C for 1 min, followed by amplification for 35 cycles (for megalin and ClC-5) or 33 cycles (for SGLT2) of 60 s at 94 °C (denaturation), 60 s at each annealing temperature (63 °C for megalin, 64°C for SGLT2, 69°C for ClC-5), and 60 s at 72 °C (extension). The PCR products were separated by electrophoresis in a 2.0% agarose gel and stained with ethidium bromide.

2.6. Western blot analysis

For Western blot analysis of megalin in HK-2 and L2 cells, whole cell lysates from the two cell lines were prepared at 7 and 4 days after seeding, respectively. After removal of the culture medium, the cells were washed and collected in the preparation buffer (150 mM NaCl, 10 mM Tris, 5 mM EDTA, pH7.4) with a cell scraper. The cell suspension was centrifuged at 8,720 g at 4°C for 5 min. After the supernatant was discarded, the cells were lysed with preparation buffer including 1% (v/v) Triton X-100, 0.1% (w/v) SDS and 1% (w/v) deoxycholic acid and

centrifuged at 8,720 g at 4°C for 5 min. The supernatant was used as a sample for immunoblotting. The sample (50 µg protein per a lane) was subjected to SDS-polyacrylamide gel electrophoresis with 6% polyacrylamide gel, and the proteins were transferred for 75 min to a polyvinylidene difluoride (PVDF) membrane at 4°C. After blotting, the membrane was blocked in 5% non-fat dry milk in Tris-buffer saline (150 mM NaCl, 20.5 mM Tris, pH7.4) containing 0.05% Tween 20 (TBS-T) and subsequently incubated with anti-megalin rabbit antiserum (1:1,000 dilution). The membrane was washed three times in TBS-T, and then incubated with HRP-linked donkey anti-rabbit IgG antibody (GE Healthcare UK Ltd., Buckinghamshire, England) (1:2,000 dilution). Then, the membrane was washed three times in TBS-T and visualized with enhanced chemiluminescence (ECL-Plus, GE Healthcare UK Ltd.). The blocking and antibody incubation processes were performed with the SNAP i.d. system (Millipore, Billerica, MA, USA).

2.7. Intracellular calcium concentration measurement

The intracellular calcium concentration levels were measured in HK-2 cells attached to the 35 mm glass bottom dish. After removal of the culture medium, the dishes were washed with HEPES buffer and incubated with HEPES buffer containing 10 µM Fura-2-AM for 40 min at 37°C. Thereafter, the cells were washed three times with HEPES buffer and incubated with HEPES buffer with or without 1 mM CaCl₂ in the chamber at room temperature (24-26°C). Fura-2 fluorescence was measured at 340 nm and 380 nm wavelengths with the ARGUS/HiSCA system (Hamamatsu Photonics, Shizuoka, Japan) equipped with a fluorescent microscope (Nikon ECLIPSE TE300; Nikon, Tokyo, Japan). The fluorescence ratio (F_{340 nm}/F_{380 nm}) is a relative index of intracellular calcium concentration. Gadolinium without or with gentamicin was added

to the dishes after the baseline reached stable, and the final concentrations of gadolinium and gentamicin were 0.3 mM and 5 mM, respectively. Ruthenium red (100 μ M) was included in the incubation buffer before gadolinium was added.

2.8. *Data analysis*

The half-maximal inhibitory concentration (IC₅₀) values were determined by fitting data with a Hill equation using the KaleidaGraphTM program (Version 3.08, Synergy Software, PA, USA). Statistically significant differences were determined by Student's *t*-test, or one way or two way analysis of variance (ANOVA) with the Tukey-Kramer's test for post hoc analysis. A *P* value less than 0.05 was considered statistically significant.

3. Results

3.1. Sodium-dependent uptake of D-[³H]glucose and L-[³H]alanine in HK-2 cells

First, we examined whether HK-2 cells employed in this study retain functional properties that are characteristic of renal proximal tubular cells. As shown in Figs. 1A and 1B, the uptakes of D-[³H]glucose and L-[³H]alanine were significantly decreased in the absence of Na⁺ in the incubation buffer. In addition, the uptakes of D-[³H]glucose and L-[³H]alanine were inhibited by an excess of each unlabeled compound. Thus, HK-2 cells have the ability to transport D-glucose and L-alanine via sodium-dependent transporter systems, which are present in the apical membrane of renal proximal tubular cells.

3.2. Expression of mRNA and protein of megalin in HK-2 cells

Next, expression of mRNA for megalin in HK-2 cells employed in this study was analyzed by RT-PCR analysis (Fig. 1C). PCR amplification for a total of 35 cycles allowed the identification of a band of the expected size on the gel, but the band from megalin mRNA was very faint. No band with the expected size was detected when the total RNA was subjected to PCR without reverse transcription. In addition, immunoblot analysis revealed little or no expression of megalin in HK-2 cell lysates, whereas megalin was clearly detected in the cell lysates from L2 rat yolk sac carcinoma cells (Fig. 1D), which have been reported to abundantly express megalin (Orlando and Farquhar, 1993). We also examined the mRNA expression of SGLT2 and CIC-5, which are expressed in renal proximal tubules (Wright, 2001; Christensen et

al., 2003). RT-PCR analysis revealed that the two genes are expressed in HK-2 cells employed in this study (Supplementary fig. S1).

3.3. Temperature-dependent uptake of [³H]gentamicin in HK-2 cells and effects of various aminoglycosides

Uptake of [³H]gentamicin at 37°C was increased with increasing the incubation time, and [³H]gentamicin uptake at 4°C was significantly lower than that at 37°C at the same incubation time (Fig. 2). Figure 3 shows the effects of various aminoglycoside antibiotics on [³H]gentamicin uptake. [³H]Gentamicin uptake was significantly inhibited by all aminoglycosides tested.

3.4. Effects of endocytosis inhibitors and a cationic peptide on [³H]gentamicin uptake in HK-2 cells and OK cells

The effects of endocytosis inhibitors on [³H]gentamicin in HK-2 cells and OK cells were compared (Table 1). The OK cells employed in this study were previously shown to express megalin (Watanabe et al., 2004). Colchicine and cytochalasin D, which inhibit endocytosis by interacting with cytoskeleton, had no significant effect on [³H]gentamicin uptake in HK-2 cells, whereas the uptake of [³H]gentamicin in OK cells was significantly inhibited by these endocytosis inhibitors. Next, the effect of N-WASP181-200, a basic peptide consisting of 20 amino acid residues, was examined. Previously, we observed that N-WASP181-200 decreased not only [³H]gentamicin uptake in OK cells but also the binding to rat renal brush-border membrane in vitro and the accumulation in rat renal cortex in vivo (Nagai et al., 2006; Watanabe

et al, 2004). However, N-WASP181-200 did not decrease [^3H]gentamicin uptake in HK-2 cells, whereas [^3H]gentamicin uptake in OK cells was significantly inhibited by N-WASP181-200 (Table 1).

3.5. Effects of cation channel blockers on [^3H]gentamicin uptake in HK-2 cells

Figure 4 shows that the effect of ruthenium red, a nonspecific TRP cation channel blocker, on [^3H]gentamicin uptake in HK-2 cells. The uptake of [^3H]gentamicin was significantly inhibited by ruthenium red at a concentration of 10 μM or higher. Furthermore, we examined the effect of gadolinium, a trivalent cation that blocks many types of cation channels, on [^3H]gentamicin uptake. Interestingly, a bell-shaped concentration-dependence was observed with a maximum increase in [^3H]gentamicin uptake at 0.3 mM of gadolinium (Fig. 5). The IC_{50} value of gadolinium was 1.7 mM when data with the range from 0.3 mM to 10 mM gadolinium were used for curve-fitting. When [^3H]gentamicin was incubated with gadolinium for 30, 60 and 120 min, the enhanced uptake of [^3H]gentamicin was clearly observed at 30 min, and it was retained up to 120 min (Fig. 6).

3.6. Effect of gadolinium on intracellular calcium concentration in HK-2 cells

Recently, gadolinium is reported to activate the vanilloid receptor TRPV1 at concentrations of 10 to 300 μM (Tousova et al., 2005). To investigate whether gadolinium stimulates calcium influx in HK-2 cells, changes in the intracellular calcium concentration, $[\text{Ca}^{2+}]_i$, was examined by ratiometric calcium imaging with Fura-2. Figure 7A shows 0.3 mM

gadolinium induced a rapid increase in $[Ca^{2+}]_i$. When 0.3 mM gadolinium was applied to the cells incubated with Ca^{2+} -free buffer, only slight increase in $[Ca^{2+}]_i$ was observed (Fig. 7B). Thus, it is likely that $[Ca^{2+}]_i$ increase by gadolinium is due to the enhanced influx of extracellular calcium, rather than release from cellular calcium stores. The enhanced effect of gadolinium on $[Ca^{2+}]_i$ was reduced by 100 μ M ruthenium red and 5 mM gadolinium (Figs. 7C and 7D).

3.7. Effect of extracellular calcium removal on gadolinium-induced stimulation of $[^3H]$ gentamicin uptake in HK-2 cells

To investigate whether gadolinium-induced increase in $[Ca^{2+}]_i$ is involved in modulation of $[^3H]$ gentamicin uptake, the effect of gadolinium on $[^3H]$ gentamicin uptake was examined in the incubation buffer in the presence or absence of calcium. As shown in Fig. 8, stimulation of $[^3H]$ gentamicin uptake by 0.5 mM gadolinium was observed under calcium-free conditions to a similar extent as that in the buffer containing 1 mM calcium. Thus, it is likely that the enhanced uptake of $[^3H]$ gentamicin by 0.5 mM gadolinium is not related with increase in $[Ca^{2+}]_i$.

3.8. Effect of ruthenium red on gadolinium-induced stimulation of $[^3H]$ gentamicin uptake in HK-2 cells

Figure 9 shows the effect of ruthenium red on $[^3H]$ gentamicin uptake in the absence or presence of 0.3 mM gadolinium. Ruthenium red inhibited $[^3H]$ gentamicin uptake enhanced by 0.3 mM gadolinium in a concentration-dependent manner. The inhibitory effect of 100 μ M ruthenium red on $[^3H]$ gentamicin uptake (the uptake value without ruthenium red minus that with

100 μ M ruthenium red) was greater in the presence of gadolinium (107.4 pmol/mg protein/120 min) than that in the absence of gadolinium (29.8 pmol/mg protein/120 min). This observation indicates that gadolinium-induced uptake of [3 H]gentamicin is ruthenium red-sensitive.

4. Discussion

The human renal proximal tubular cell line HK-2, derived from the healthy kidney of an adult male (Ryan et al., 1994), is commonly used as a suitable in vitro model to study renal physiology and pathology. Though there are several reports concerning gentamicin-induced changes in cellular functions employing HK-2 cells (Zhipeng et al., 2006; Zager et al., 2007; Park et al., 2010), the mechanisms underlying cellular uptake of gentamicin in HK-2 cells has not been clarified. In this study, the uptake mechanism of gentamicin in HK-2 cells was characterized.

When HK-2 cells were first established by Ryan et al. (1994), the cells were cultured in the keratinocyte serum-free medium supplemented with epidermal growth factor and bovine pituitary extract. Subsequently, in addition to the original culture medium, different culture media such as Dulbecco's modified Eagle's medium (DMEM) and DMEM/nutrient Ham's mixture F-12 (DMEM/F-12) have been employed for maintaining the cell line. In this study, HK-2 cells were cultured in DMEM/F-12 containing 10% fetal bovine serum, which has been employed by several other groups (Holthouser et al., 2010, Park et al., 2010, Wen et al., 2010). We first examined whether the HK-2 cells retain functional characteristics of renal proximal tubular cells. The uptakes of D-[³H]glucose and L-[³H]alanine in HK-2 cells were shown to be sodium-dependent. The observations indicate that the HK-2 cells retain sodium-coupled transport systems for sugars and amino acids, which are characteristic of the apical membrane of the renal proximal tubular cells (Wright 2001, Pinho et al., 2010, Bailey 2011). Thus, we confirmed that the HK-2 cells used in this study retain functional characteristics of the renal proximal tubular cells.

Megalin is a multiligand endocytic receptor abundantly expressed in the renal proximal tubule (Christensen and Birn, 2002; Christensen et al., 2009). It has been shown that megalin

plays a crucial role in renal accumulation of gentamicin under in vivo and in vitro conditions (Moestrup et al., 1995; Nagai et al., 2001; Schmitz et al., 2002). Surprisingly, HK-2 cells employed in this study had very slight expression of megalin mRNA and protein. These observations were inconsistent with other results that reported the clear expression of megalin protein in HK-2 cells (Gildea et al., 2010; Li et al., 2008; Oroszlán et al., 2010). It is unknown at present why there are differences in expression of megalin in HK-2 cells between our laboratory and others, but the expression level of megalin might be due to the differences in culture conditions.

In this study, the uptake mechanism of [^3H]gentamicin in HK-2 cells were characterized and compared with that in OK cells, a renal proximal tubular cell line expressing megalin (Zhai et al., 2000; Watanabe et al., 2004). Though temperature-dependent uptake of [^3H]gentamicin was observed in both cell lines, general endocytosis inhibitors such as colchicine and cytochalasin D significantly decreased [^3H]gentamicin in OK cells, but not in HK-2 cells. These observations suggest that [^3H]gentamicin uptake in HK-2 cells is endocytosis-independent, in contrast with endocytosis-dependent uptake of [^3H]gentamicin in OK cells. Furthermore, a cationic 20-amino acid residue peptide N-WASP181-200, which inhibited [^3H]gentamicin uptake in OK cells in this and our previous studies (Watanabe et al., 2004), had no effect on the uptake of [^3H]gentamicin in HK-2 cells. Thus, it is likely that the molecular mechanism of [^3H]gentamicin uptake in HK-2 is distinct from that in OK cells, especially concerning the involvement of endocytosis pathway. In LLC-PK₁, a pig kidney epithelial cell line, gentamicin uptake was inhibited by cytochalasin B and colchicine, indicating that gentamicin is taken up by an endocytic pathway in LLC-PK₁ cells (Hori et al., 1992). Since LLC-PK₁ cells is reported to express megalin (Nielsen et al., 1998), megalin may play an important role in the endocytosis-dependent uptake of gentamicin in LLC-

PK₁ cells. Taken together, the differences in the molecular mechanisms of gentamicin uptake among these cell lines might result from those in the expression levels of megalin.

Though [³H]gentamicin uptake in HK-2 cells was shown to be endocytosis-independent, the uptake was temperature-dependent, and was inhibited by other aminoglycoside antibiotics including unlabeled gentamicin, kanamycin and streptomycin (Figs. 2 and 3). Therefore, a molecule mediating the cellular uptake of gentamicin in HK-2 cells might be involved. Recently, Mydral and Steyger (2005) reported that ruthenium red, a nonspecific TRP channel inhibitor, decreased the uptake of Texas Red-conjugated gentamicin in MDCK cells, a canine kidney distal tubule cell line. Like MDCK cells, ruthenium red significantly inhibited [³H]gentamicin uptake in HK-2 cells. Furthermore, they reported that gadolinium, a mechanosensitive channel blocker inhibited Tex Red-conjugated gentamicin uptake in MDCK cells in a concentration-dependent manner (0.5, 5 and 50 mM gadolinium). However, in contrast with the observations in MDCK cells, we observed that gadolinium displayed a bell-shaped concentration-dependence with a maximum increase (380% of control) at 0.3 mM. Thus, the molecular mechanism on gentamicin uptake in HK-2 cells may not be necessarily the same as that in MDCK cells. This might result from the differences in cation channel member(s) mediating gentamicin uptake in each cell line.

Saito et al. (1986) reported that A23187, a calcium ionophore, stimulated gentamicin uptake in LLC-PK₁ cells, suggesting that calcium ion movement into the cells might be associated with the transport mechanism of gentamicin in the LLC-PK₁ cells. In the present study, gadolinium was observed to increase [Ca²⁺]_i in HK-2 cells (Fig. 7A), indicating that gadolinium activates calcium channel(s) in HK-2 cells. To investigate whether the increase in [Ca²⁺]_i is involved in the enhanced uptake of gentamicin by gadolinium, we examined the effect of gadolinium on [³H]gentamicin uptake in HK-2 cells under calcium-free conditions. Removal of calcium from the incubation buffer did not attenuate the gadolinium-induced stimulation of

[³H]gentamicin uptake, though the gadolinium-induced increase in [Ca^{2+}]_i almost disappeared under calcium-free conditions. Thus, the effect of gadolinium on [³H]gentamicin uptake in HK-2 cells was independent of the increase in [Ca^{2+}]_i by gadolinium. These observations might further support the suggestion that the molecular mechanisms of gentamicin uptake are different between LLC-PK₁ cells and HK-2 cells as described above.

In conclusion, we found that [³H]gentamicin was taken up via an endocytosis-independent pathway in HK-2 cells, in which the expression level of megalin was very low. In addition, gadolinium biphasically modulated the uptake of [³H]gentamicin in HK-2 cells. These results suggest that the cellular uptake of gentamicin might vary greatly according to the expression and functional levels of a molecule mediating gentamicin entry into cells.

Acknowledgments

We thank the Analysis Center of Life Science, Natural Science Center for Basic Research and Development, Hiroshima University, for the use of their facilities. This work was supported in part by a Grant-in-Aid for Scientific Research from the Ministry of Education, Culture, Sports, Science and Technology in Japan.

References

- Bailey, C.J., 2011. Renal glucose reabsorption inhibitors to treat diabetes. *Trends Pharmacol. Sci.* 32, 63-71.
- Bradford, M.M., 1976. A rapid and sensitive method for the quantitation of microgram quantities of protein utilizing the principle of protein-dye binding. *Anal. Biochem.* 72, 248-254.
- Christensen, E.I., Birn, H., 2002. Megalin and cubilin: multifunctional endocytic receptors. *Nat. Rev. Mol. Cell Biol.* 3, 256-266.
- Christensen, E.I., Verroust, P.J., Nielsen, R., 2009. Receptor-mediated endocytosis in renal proximal tubule. *Pflugers Arch.* 458, 1039-1048.
- Christensen, E.I., Nielsen, S., Moestrup, S.K., Borre, C., Maunsbach, A.B., de Heer, E., Ronco, P., Hammond, T.G., Verroust, P., 1995. Segmental distribution of the endocytosis receptor gp330 in renal proximal tubules. *Eur. J. Cell Biol.* 66, 349-364.
- Christensen, E.I., Devuyst, O., Dom, G., Nielsen, R., Van der Smissen, P., Verroust, P., Leruth, M., Guggino, W.B., Courtoy, P.J., 2003. Loss of chloride channel ClC-5 impairs endocytosis by defective trafficking of megalin and cubilin in kidney proximal tubules. *Proc. Natl. Acad. Sci. USA* 100, 8472-8477.
- Gildea, J.J., Shah, I., Weiss, R., Casscells, N.D., McGrath, H.E., Zhang, J., Jones, J.E., Felder, R.A., 2010. HK-2 human renal proximal tubule cells as a model for G protein-coupled

receptor kinase type 4-mediated dopamine 1 receptor uncoupling. *Hypertension* 56, 505-511.

Holthouser, K.A., Mandal, A., Merchant, M.L., 2010. Schelling JR, Delamere NA, Valdes RR Jr, Tyagi SC, Lederer ED, Khundmiri SJ. Ouabain stimulates Na-K-ATPase through a sodium/hydrogen exchanger-1 (NHE-1)-dependent mechanism in human kidney proximal tubule cells. *Am. J. Physiol. Renal Physiol.* 299, F77-F90.

Hori, R., Okuda, M., Ohishi, Y., Yasuhara, M., Takano, M., 1992. Surface binding and intracellular uptake of gentamicin in the cultured kidney epithelial cell line (LLC-PK₁). *J. Pharmacol. Exp. Ther.* 261, 1200-1205.

Iwata, M., Zager, R.A., 1996. Myoglobin inhibits proliferation of cultured human proximal tubular (HK-2) cells. *Kidney Int.* 50, 796-804.

Karasawa, T., Wang, Q., Fu, Y., Cohen, D.M., 2008. Steyger PS. TRPV4 enhances the cellular uptake of aminoglycoside antibiotics. *J Cell Sci.* 121, 2871-2879.

Li, M., Balamuthusamy, S., Simon, E.E., Batuman, V., 2008. Silencing megalin and cubilin genes inhibits myeloma light chain endocytosis and ameliorates toxicity in human renal proximal tubule epithelial cells. *Am. J. Physiol. Renal Physiol.* 295, F82-F90.

Lopez-Novoa, J.M., Quiros, Y., Vicente, L., Morales, A.I., Lopez-Hernandez, F.J., 2011. New insights into the mechanism of aminoglycoside nephrotoxicity: an integrative point of view. *Kidney Int.* 79, 33-45.

- Mingeot-Leclercq, M.P., Tulkens, P.M., 1999. Aminoglycosides: nephrotoxicity. *Antimicrob. Agents Chemother.* 43, 1003-1012.
- Moestrup, S.K., Cui, S., Vorum, H., Bregengård, C., Bjørn, S.E., Norris, K., Gliemann, J., Christensen, E.I., 1995. Evidence that epithelial glycoprotein 330/megalin mediates uptake of polybasic drugs. *J. Clin. Invest.* 96, 1404-1413.
- Molitoris, B.A., Meyer, C., Dahl, R., Geerdes, A., 1993. Mechanism of ischemia-enhanced aminoglycoside binding and uptake by proximal tubule cells. *Am. J. Physiol.* 264, F907-F916.
- Myrdal, S.E., Steyger, P.S., 2005. TRPV1 regulators mediate gentamicin penetration of cultured kidney cells. *Hear Res.* 204, 170-182.
- Myrdal, S.E., Johnson, K.C., Steyger, P.S., 2005. Cytoplasmic and intra-nuclear binding of gentamicin does not require endocytosis. *Hear. Res.* 204, 156-169.
- Nagai, J., Takano, M., 2004. Molecular aspects of renal handling of aminoglycosides and strategies for preventing the nephrotoxicity. *Drug Metab. Pharmacokinet.* 19, 159-170.
- Nagai, J., Tanaka, H., Nakanishi, N., Murakami, T., Takano, M., 2001. Role of megalin in renal handling of aminoglycosides. *Am J Physiol Renal Physiol.* 281, F337-F344.
- Nagai, J., Saito, M., Adachi, Y., Yumoto, R., Takano, M., 2006. Inhibition of gentamicin binding to rat renal brush-border membrane by megalin ligands and basic peptides. *J. Control. Release* 112, 43-50.

- Nielsen, R., Birn, H., Moestrup, S.K., Nielsen, M., Verroust, P., Christensen, E.I., 1998. Characterization of a kidney proximal tubule cell line, LLC-PK₁, expressing endocytotic active megalin. *J. Am. Soc. Nephrol.* 9, 1767-1776.
- Orlando, R.A., Farquhar, M.G., 1993. Identification of a cell line that expresses a cell surface and a soluble form of the gp330/receptor-associated protein (RAP) Heymann nephritis antigenic complex. *Proc. Natl. Acad. Sci. USA* 90, 4082-4086.
- Oroszlán, M., Bieri, M., Ligeti, N., Farkas, A., Meier, B., Marti, H.P., Mohacsi, P., 2010. Sirolimus and everolimus reduce albumin endocytosis in proximal tubule cells via an angiotensin II-dependent pathway. *Transpl. Immunol.* 23, 125-132.
- Park, J.W., Bae, E.H., Kim, I.J., Ma, S.K., Choi, C., Lee, J., Kim, S.W., 2010. Renoprotective effects of paricalcitol on gentamicin-induced kidney injury in rats. *Am. J. Physiol. Renal Physiol.* 298, F301-F313.
- Pinho, M.J., Cabral, J.M., Silva, E., Serrão, M.P., Soares-da-Silva, P., 2011. LAT1 overexpression and function compensates downregulation of ASCT2 in an in vitro model of renal proximal tubule cell ageing. *Mol. Cell. Biochem.* 349, 107-116.
- Ryan, M.J., Johnson, G., Kirk, J., Fuerstenberg, S.M., Zager, R.A., Torok-Storb, B., 1994. HK-2: an immortalized proximal tubule epithelial cell line from normal adult human kidney. *Kidney Int.* 45, 48-57.
- Saito, H., Inui, K., Hori, R., 1986. Mechanisms of gentamicin transport in kidney epithelial cell line (LLC-PK₁). *J. Pharmacol. Exp. Ther.* 238, 1071-1076.

- Sastrasinh, M., Knauss, T.C., Weinberg, J.M., Humes, H.D., 1982. Identification of the aminoglycoside binding site in rat renal brush border membranes. *J. Pharmacol. Exp. Ther.* 222, 350-358.
- Schacht, J., 1979. Isolation of an aminoglycoside receptor from guinea pig inner ear tissues and kidney. *Arch. Otorhinolaryngol.* 224, 129-134.
- Schmitz, C., Hilpert, J., Jacobsen, C., Boensch, C., Christensen, E.I., Luft, F.C., Willnow, T.E., 2002. Megalin deficiency offers protection from renal aminoglycoside accumulation. *J. Biol. Chem.* 277, 618-622.
- Servais, H., Ortiz, A., Devuyst, O., Denamur, S., Tulkens, P.M., Mingeot-Leclercq, M.P., 2008. Renal cell apoptosis induced by nephrotoxic drugs: cellular and molecular mechanisms and potential approaches to modulation. *Apoptosis.* 13, 11-32.
- Stepanyan, R.S., Indzhukulian, A.A., Vélez-Ortega, A.C., Boger, E.T., Steyger, P.S., Friedman, T.B., Frolenkov, G.I., 2011. TRPA1-Mediated Accumulation of Aminoglycosides in Mouse Cochlear Outer Hair Cells. *J. Assoc. Res. Otolaryngol.* in press.
- Takano, M., Ohishi, Y., Okuda, M., Yasuhara, M., Hori, R., 1994. Transport of gentamicin and fluid-phase endocytosis markers in the LLC-PK₁ kidney epithelial cell line. *J. Pharmacol. Exp. Ther.* 268, 669-674.
- Tousova, K., Vyklicky, L., Susankova, K., Benedikt, J., Vlachova, V., 2005. Gadolinium activates and sensitizes the vanilloid receptor TRPV1 through the external protonation sites. *Mol. Cell. Neurosci.* 30, 207-217.

- Vandewalle, A., Farman, N., Morin, J.P., Fillastre, J.P., Hatt, P.Y., Bonvalet, J.P., 1981. Gentamicin incorporation along the nephron: autoradiographic study on isolated tubules. *Kidney Int.* 19, 529-539.
- Watanabe, A., Nagai, J., Adachi, Y., Katsube, T., Kitahara, Y., Murakami, T., Takano, M., 2004. Targeted prevention of renal accumulation and toxicity of gentamicin by aminoglycoside binding receptor antagonists. *J. Control. Release* 95, 423-433.
- Wedeen, R.P., Batuman, V., Cheeks, C., Marquet, E., Sobel, H., 1983. Transport of gentamicin in rat proximal tubule. *Lab. Invest.* 48, 212-223.
- Wen, Q., Huang, Z., Zhou, S.F., Li, X.Y., Luo, N., Yu, X.Q., 2010. Urinary proteins from patients with nephrotic syndrome alters the signalling proteins regulating epithelial-mesenchymal transition. *Nephrology (Carlton)*. 15, 63-74.
- Wright, E.M., 2001. Renal Na⁺-glucose cotransporters. *Am. J. Physiol. Renal Physiol.* 280, F10-F18.
- Zager, R.A., Johnson, A.C., Geballe, A., 2007. Gentamicin suppresses endotoxin-driven TNF- α production in human and mouse proximal tubule cells. *Am. J. Physiol. Renal Physiol.* 293, F1373-F1380.
- Zhai, X.Y., Nielsen, R., Birn, H., Drumm, K., Mildenerger, S., Freudinger, R., Moestrup, S.K., Verroust, P.J., Christensen, E.I., Gekle, M., 2000. Cubilin- and megalin-mediated uptake of albumin in cultured proximal tubule cells of opossum kidney. *Kidney Int.* 58, 1523-1533.

Zhipeng, W., Li, L., Qibing, M., Linna, L., Yuhua, R., Rong, Z., 2006. Increased expression of heat shock protein (HSP)72 in a human proximal tubular cell line (HK-2) with gentamicin-induced injury. *J. Toxicol. Sci.* 31, 61-70.

Figure legends

Fig. 1. General characteristics of HK-2 cells employed in this study. (A, B) Sodium-dependent uptake of D-[³H]glucose (A) and L-[³H]alanine (B) by confluent monolayers of HK-2 cells. The uptake of D-[³H]glucose (1 mM) and L-[³H]alanine (1 mM) for 20 min at 37°C was measured in the incubation buffer (control), sodium-free buffer and the incubation buffer containing 9 mM unlabeled each substrate. Each column represents the mean \pm S.E.M. of three monolayers.

* $P < 0.05$, significantly different from the value of each control by one-way analysis of variance (ANOVA) with Tukey-Kramer's post hoc test. (C) PCR amplification of megalin mRNA in HK-2 cells. Total RNA from HK-2 cells was reverse-transcribed and first-strand cDNA synthesized was amplified with a set of specific primers described in Materials and methods. The PCR products with or without reverse transcription were separated by electrophoresis through a 2% agarose gel and stained with ethidium bromide. Note that the band was from samples in the 35-cycle amplification. (D) Western blot analysis of megalin in lysates from HK-2 and L2 cells. Fifty micrograms of cell lysates were separated 6% SDS-polyacrylamide gel electrophoresis, transferred to a membrane. Megalin was detected by Western blotting with anti-megalin antiserum.

Fig. 2. Time- and temperature-dependence of [³H]gentamicin uptake by HK-2 cells. The uptake of [³H]gentamicin (10 μ M) by confluent monolayers of HK-2 cells was measured at 37°C or 4°C for indicated periods. Each symbol represents the mean \pm S.E.M. of five to six monolayers.

* $P < 0.05$, significantly different from the value at 37°C at each incubation time by one-way ANOVA with Tukey-Kramer's post hoc test.

Fig. 3. Effects of various aminoglycoside antibiotics on [³H]gentamicin uptake by HK-2 cells.

The uptake of [³H]gentamicin (10 µM) for 120 min at 37°C was measured in the absence or presence of aminoglycoside antibiotic (10 mM except 20 mM for SM and 6.5 mM for TOB).

Each symbol represents the mean ± S.E.M. of three monolayers. **P*<0.05, significantly different from the value of control by one-way ANOVA with Tukey-Kramer's post hoc test. GM, gentamicin; KM, kanamycin; SM, streptomycin; Neo, neomycin; AMK, amikacin; TOB, tobramycin; ABK, arbekacin.

Fig. 4. Concentration-dependent effect of ruthenium red on [³H]gentamicin uptake by HK-2 cells.

The uptake of [³H]gentamicin (10 µM) for 120 min at 37°C was measured in the absence or presence of ruthenium red (0.01 to 100 µM). Each symbol represents the mean ± S.E.M. of three monolayers. **P*<0.05, significantly different from the value of control by one-way ANOVA with Tukey-Kramer's post hoc test.

Fig. 5. Concentration-dependent effect of gadolinium on [³H]gentamicin uptake by HK-2 cells.

The uptake of [³H]gentamicin (10 µM) for 120 min at 37°C was measured in the absence or presence of gadolinium (0.03 to 10 mM). Each symbol represents the mean ± S.E.M. of three monolayers. **P*<0.05, significantly different from the value of control by one-way ANOVA with Tukey-Kramer's post hoc test.

Fig. 6. Time-course of the effect of gadolinium on [³H]gentamicin uptake by HK-2 cells. The uptake of [³H]gentamicin (10 µM) by confluent monolayers of HK-2 cells was measured in the

absence or presence of 0.3 mM gadolinium at 37°C for indicated periods. Each symbol represents the mean \pm S.E.M. of three monolayers. * P <0.05, significantly different from the value without 0.3 mM gadolinium at each incubation time by one-way ANOVA with Tukey-Kramer's post hoc test.

Fig. 7. Effect of gadolinium on intracellular free calcium concentration in HK-2 cells. HK-2 cells were loaded with 10 μ M Fura-2-AM, and changes in the fluorescence ratio (F340/F380 excitation) were measured to assess changes in the intracellular Ca^{2+} concentration ($[\text{Ca}^{2+}]_i$) at room temperature (24~26°C). (A) $[\text{Ca}^{2+}]_i$ was increased by addition of gadolinium (0.3 mM) in normal incubation buffer containing 1 mM Ca^{2+} . (B) The gadolinium-induced $[\text{Ca}^{2+}]_i$ changes in Ca^{2+} -free buffer was markedly decreased. (C) Ruthenium red (100 μ M) decreased the enhanced effect of gadolinium (0.3 mM) on $[\text{Ca}^{2+}]_i$, but it did not completely inhibit the changes in $[\text{Ca}^{2+}]$ by gadolinium. (D) Simultaneous addition of gadolinium (0.3 mM) and gentamicin (5 mM) decreased the changes in $[\text{Ca}^{2+}]_i$ compared to that of 0.3 mM gadolinium alone.

Fig. 8. Effect of removal of extracellular calcium on gadolinium-induced stimulation of $[\text{}^3\text{H}]$ gentamicin uptake by HK-2 cells. The uptake of $[\text{}^3\text{H}]$ gentamicin (10 μ M) for 120 min at 37°C in the incubation buffer with (open column) or without (gray column) 1 mM Ca^{2+} was measured in the absence or presence of 0.5 mM gadolinium. Each column represents the mean \pm S.E.M. of three monolayers. Asterisks indicate statistically significant (P <0.05) as determined by two way ANOVA with Tukey-Kramer's post hoc test.

Fig. 9. Concentration-dependent effect of ruthenium red on gadolinium-induced stimulation of [³H]gentamicin uptake by HK-2 cells. The uptake of [³H]gentamicin (10 μM) without (open circle) or with (closed circle) of 0.3 mM gadolinium was measured in the absence (control) or presence of ruthenium red (10, 30 and 100 μM) for 120 min at 37°C. Each symbol represents the mean ± S.E.M. of three monolayers. **P*<0.05, significantly different from the value of each control. †*P*<0.05, significantly different from the value in the presence of 0.3 mM gadolinium with the same concentration of ruthenium red. Statistical analysis was performed using two-way ANOVA with Tukey-Kramer's post hoc test.

Table 1. Effects of colchicine, cytochalasin D and N-WASP181-200 on [^3H]gentamicin uptake in HK-2 cells and OK cells.

Inhibitors	[^3H]Gentamicin uptake (% of control)	
	HK-2 cells	OK cells
100 μM colchicine	108.7 \pm 9.6	64.3 \pm 1.3 ^a
20 μM cytochalasin D	119.5 \pm 12.5	64.2 \pm 2.6 ^a
100 μM N-WASP181-200	102.4 \pm 10.3	39.2 \pm 2.2 ^a

The uptake of [^3H]gentamicin (10 μM) at 37°C was measured in the absence (control) or presence of 100 μM colchicine, 20 μM cytochalasin D or 100 μM N-WASP181-200. Each value represents the mean \pm S.E.M. of three monolayers. ^a $P < 0.05$, significantly different from the value of each control by Student's *t*-test. The uptake values for control in HK-2 cells and OK cells were 58.8 \pm 4.8 pmol/mg protein/120 min and 104.5 \pm 7.5 pmol/mg protein/60 min, respectively.

Figure 1

Fig. 1

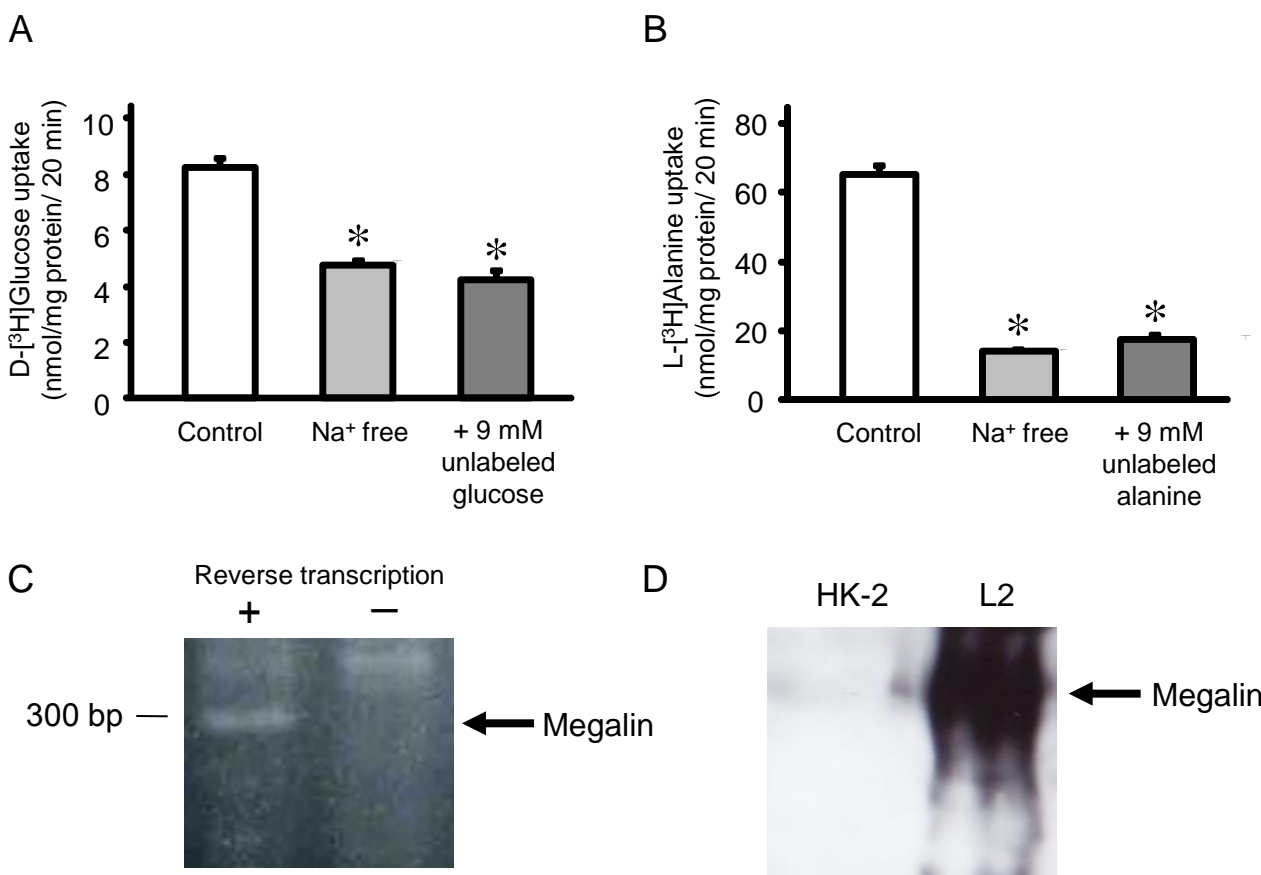


Figure 2

Fig. 2

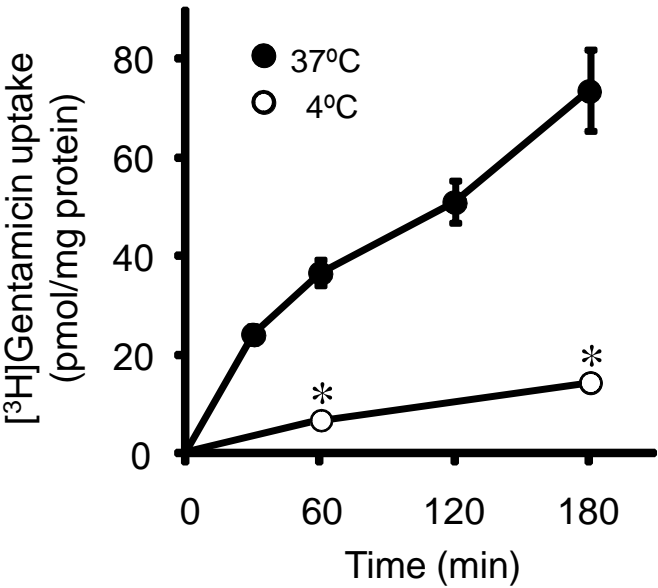


Fig. 3

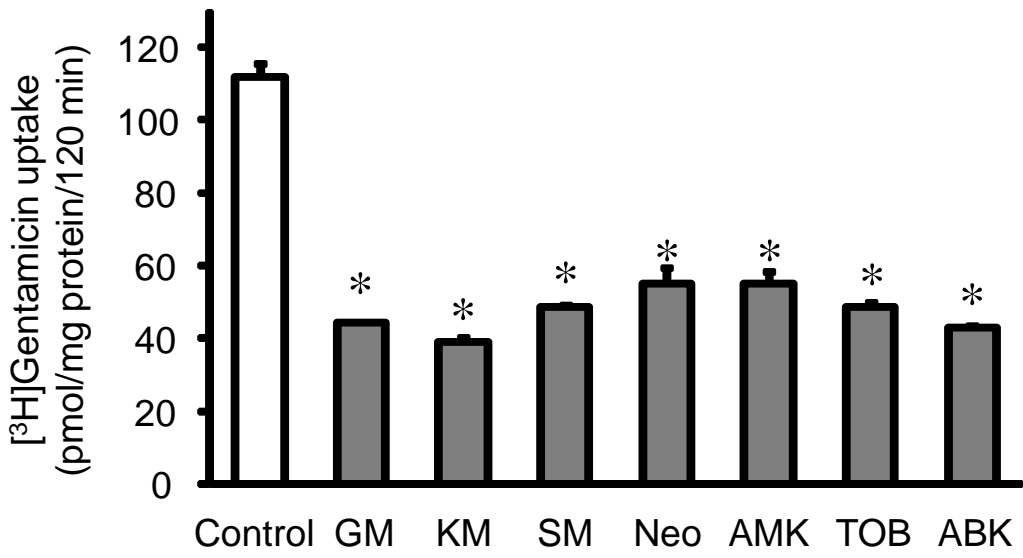


Figure 4

Fig. 4

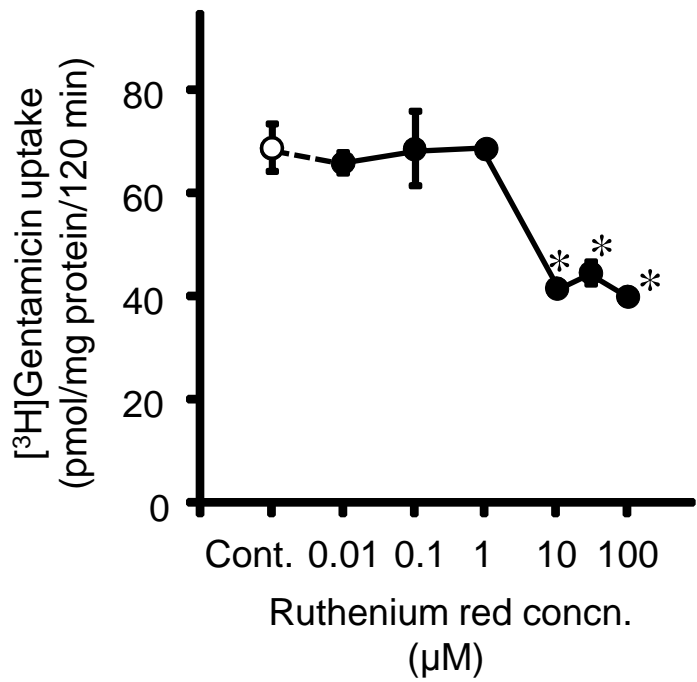


Figure 5

Fig. 5

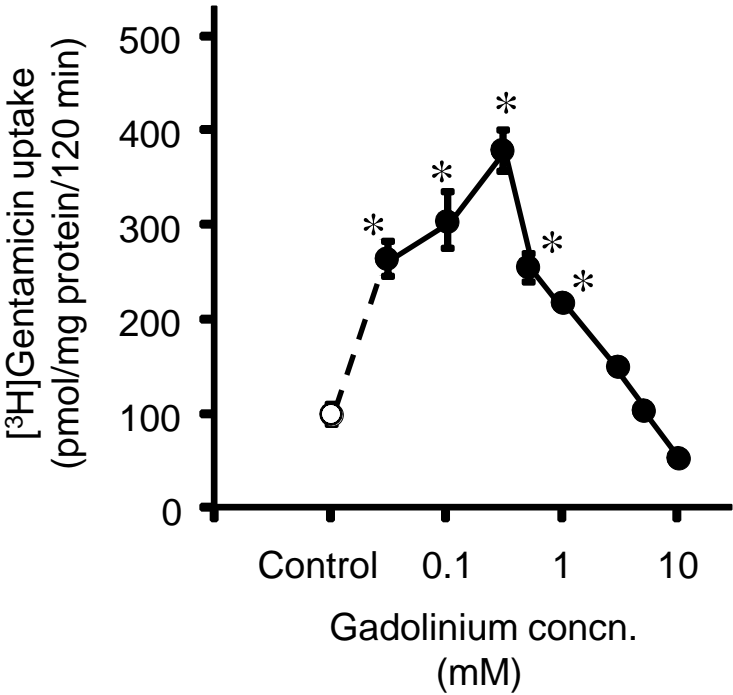


Figure 6

Fig. 6

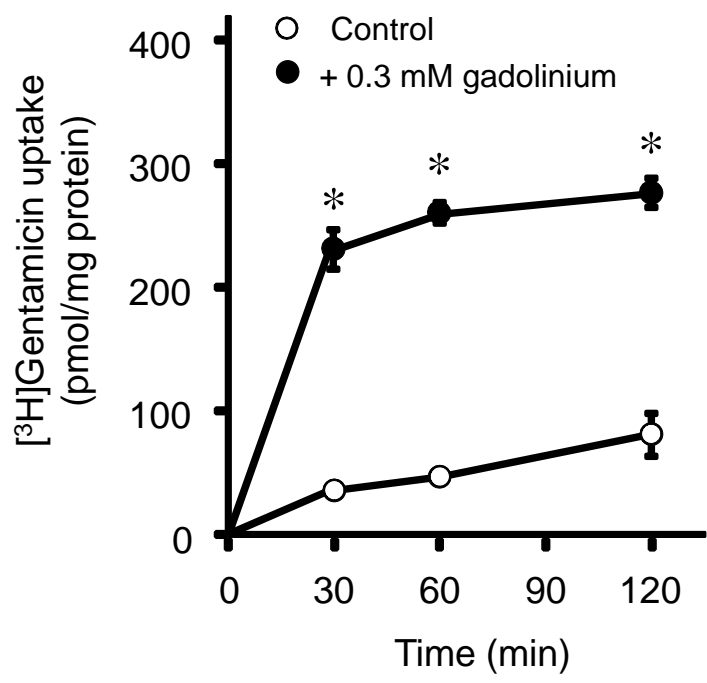


Fig. 7

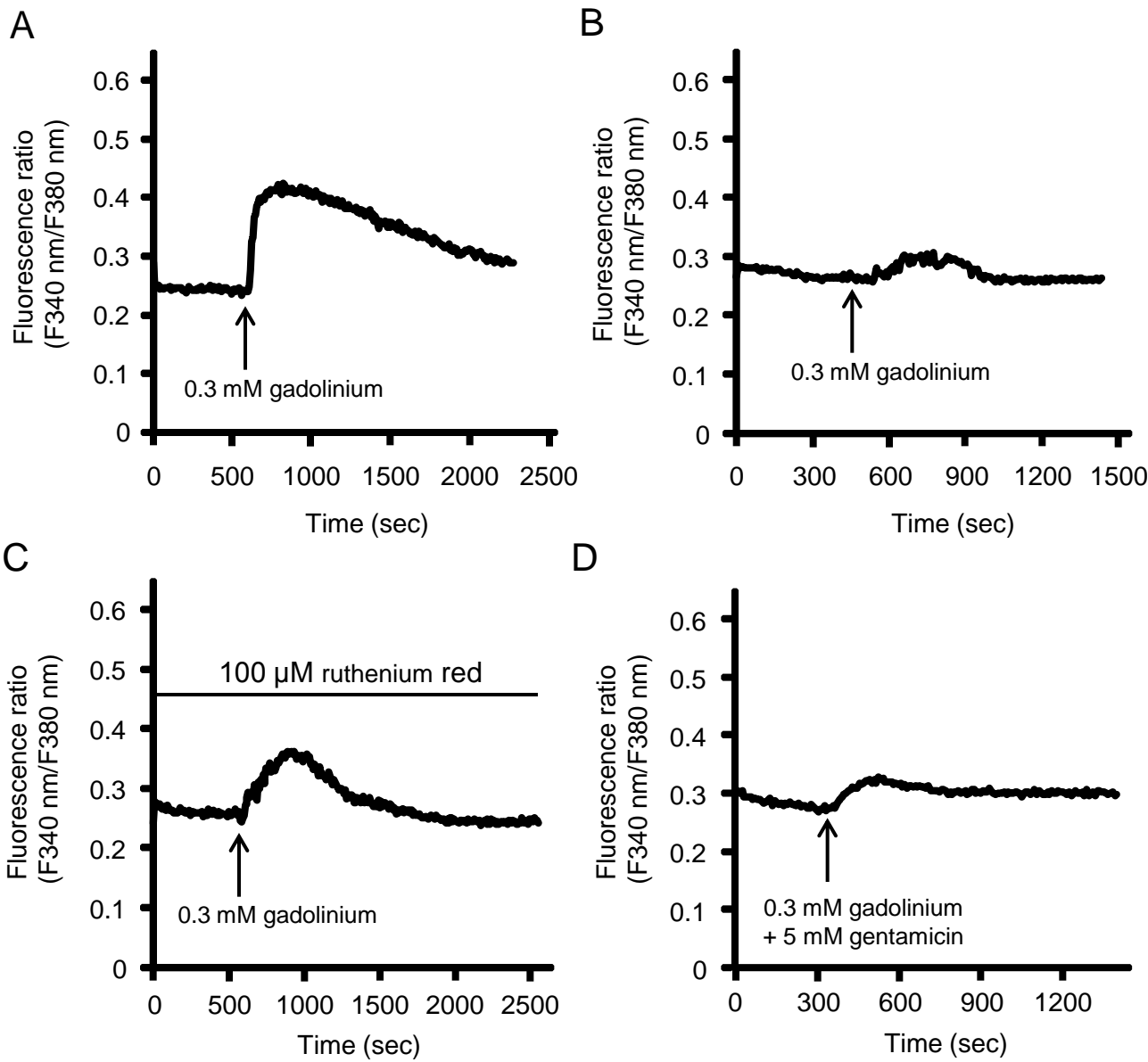


Figure 8

Fig. 8

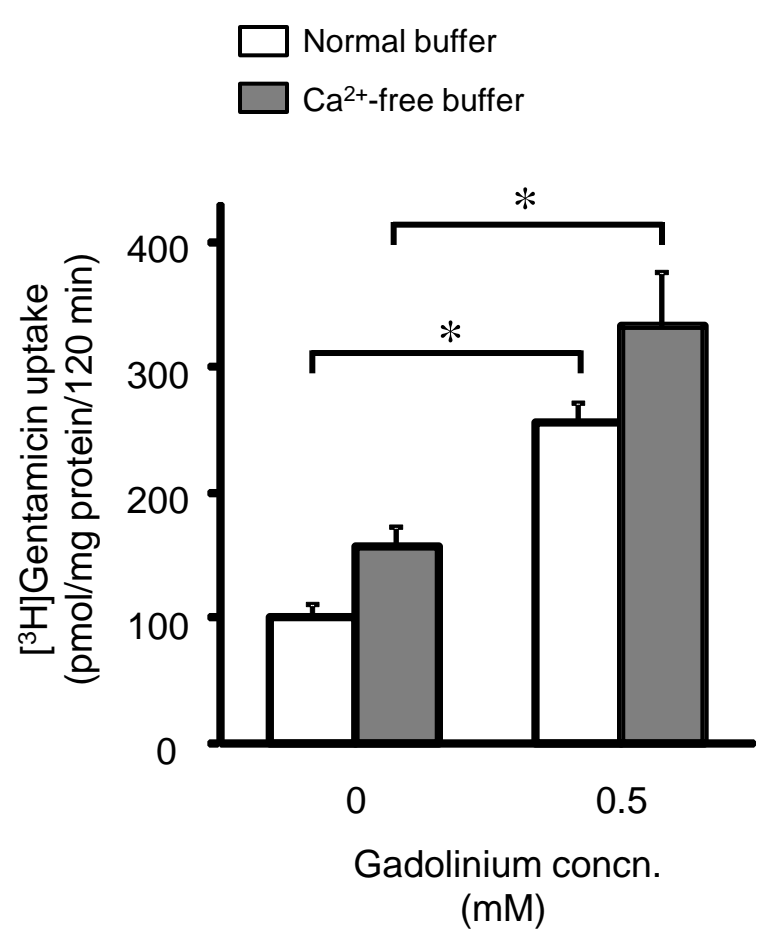
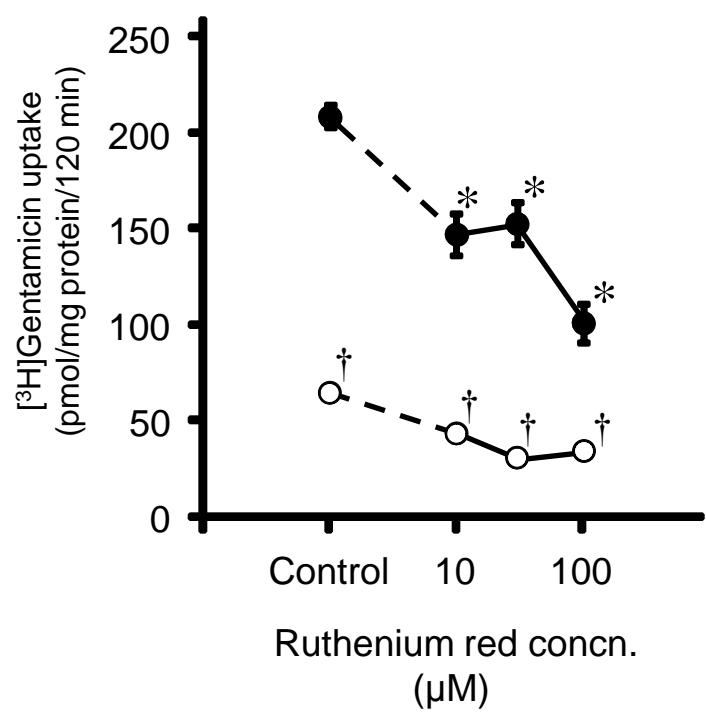


Figure 9

Fig. 9



Supplementary material for online publication only

[Click here to download Supplementary material for online publication only: Suppl. fig. 1.ppt](#)